Application of Wiener Filter and Sparsity Theory for Pulse Unfolding from Scintillator Detector

1st Tiago Quirino
dept. Electrical Eng.
Rio de Janeiro State University
Rio de Janeiro, Brazil
tiago.quirino@cern.ch

2nd Guilherme Cit
Electronic Eng. Post-Graduation Program
State University of Rio de Janeiro
Rio de Janeiro, Brazil
guilhermecit@gmail.com

3rd Gabriel Cesário
dept. Electronics and Telecomm. Eng.
State University of Rio de Janeiro
Rio de Janeiro, Brazil
silva.gabriel_41@graduacao.uerj.br

4th Sérgio Inácio
Mech. Eng. Post-Graduation Program
State University of Rio de Janeiro
Rio de Janeiro, Brazil
diamagneto@gmail.com

5th Antonio Pereira
dept. High Energy Physics
State University of Rio de Janeiro
Rio de Janeiro, Brazil
antonio.vilela.pereira@cern.ch

6th André Massafferri
COHEP
Brazilian Center for Physics Research
Rio de Janeiro, Brazil
massafferri@cbpf.br

7th Luciano Manhães
dept. Electrical Eng.
Federal University of Juiz de Fora
Juiz de Fora, Brazil
luciano.manhaes.de.andrade.filho@cern.ch

8th Diogo Rocha
COHEP
Brazilian Center for Physics Research
Rio de Janeiro, Brazil
diogo-ayres@hotmail.com

9th Jorge Amaral
dept.Elec.and Telecomm. Eng.
State University of Rio de Janeiro
Rio de Janeiro, Brazil
jamaral@eng.uerj.br

Abstract—**This study introduces an unfolding algorithm that integrates the Wiener Filter and Sparsity theory to effectively narrow the width of pulses in time, addressing the challenge of pile-up effects in environments with substantial electronic noise. The algorithm is tested with data from cosmic ray setup experiment that is composed by a scintillator and a silicon photomultiplier (SiPM). The algorithm's performance highlights its potential in improving the consistency of peak positioning and pulse resolution, crucial for precise radiation measurement.**

Index Terms—**Digital Filter, Scintillator Detector, Sparsity Theory, Wiener Filter**

I. INTRODUCTION

Scintillation detectors are transitioning from the traditional use of photomultiplier tubes (PMTs) to employing Silicon Photomultipliers (SiPMs) for light collection in some applications [1, 2]. Both devices are highly sensitive to light, capable of millions in internal gain, and can generate electrical pulses in response to particle detection. However, SiPMs offer advantages such as lower operating voltage and reduced size, making them ideal for modern applications, although they are very susceptible to noise [3].

The susceptibility of SiPMs to noise can be a significant challenge, particularly in cosmic rays detection, where precision in measuring light is critical for accurately determining the energy of the detected particle. To mitigate these effects, signal conditioning techniques are employed analogically to attenuate noise [1].

Another reason for utilizing the signal conditioning circuit relates to the intrinsic waveform characteristics of SiPM-based detectors, which are marked by very short rise and fall times on the order of a few nanoseconds. The brief duration of these pulses poses a substantial challenge for instrumentation development, as digitizing such short-duration pulses necessitates a sampling rate that is either technologically or economically unfeasible. Advantageously, the same signal conditioning approach that enhances the signal in noise also performs pulse stretching. This extension of the pulse duration effectively reduces the requisite sampling rate, easing the technological demands of the detection system [4].

While signal conditioning is essential for reducing noise and improving data analysis, it can inadvertently affect extracting critical features such as amplitude, mainly due to the pile-up effect. This effect occurs when the signal widens in time; a common strategy to reduce noise increases the likelihood of event overlap. Such pile-up can distort the measured amplitude compared to the actual signal amplitude, as illustrated in Figure 1 [4]. Therefore, it is crucial that the signal conditioning circuit design carefully balances the need for pulse extension to reduce noise with the need to minimize pile-up.

However, the unfolding technique will mitigate these challenges and enhance the analysis process. This study focuses on accurately estimating signal peaks, which are critical for precise energy measurements in various detector applications. By digitally narrowing the pulses, the unfolding technique removes the posterior unwanted effects of widening introduced by the conditioning circuit, thus recovering the original signal
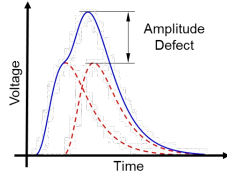
Fig. 1. Pile-up effect.

Fig. 2. Block diagram of detector readout chain.

characteristics.

The effectiveness of unfolding techniques in correcting signal distortions and improving the reliability of measured data as demonstrated by Jordanov [5, 6], Difulvio [7] and Zeng [8], who have shown the effectiveness of unfolding method in correcting signal distortions and improving the reliability of measured data in comparable contexts.

Specifically, the unfolding proposal involves the use of an optimal linear filtering algorithm, the Wiener filter, followed by a nonlinear function derived from sparsity theory, as similarly employed in previous work [9].

An experimental setup was utilized to verify the unfolding algorithm. This setup consists of a scintillator coupled to a SiPM to detect cosmic rays. The scintillator converts the energy of cosmic rays into photons of light, which are subsequently detected by the SiPM, resulting in electrical pulses. The signal conditioning circuit then processes these pulses. While this setup proves effective, it also introduces additional complexities in pulse analysis due to the modifications imposed by the signal processing circuit. These challenges have motivated the development and application of the unfolding method, which will be explored in detail in subsequent sections of this article. The organization of the paper is as follows. Section II describes the instrumentation system for particle detection. Section III details the unfolding method for measurement compensation. Section IV describes the experimental procedure and discusses the results, and finally, Section V concludes the paper with final remarks and future work notes.

II. INSTRUMENTATION SYSTEMS FOR PARTICLE DETECTION ANS MEASUREMENT

Pulse detectors are essential measuring instruments in high-energy physics, astronomy, and nuclear physics, among others. They can interact with short-duration phenomena, such as particle interactions, and provide corresponding electrical pulses, albeit with low electrical charge. These devices often employ scintillators optically coupled to photomultipliers, with SiPMs being a widely adopted choice due to their lower supply voltage and compactness advantages [4].

The instrumentation of these detectors requires systems that include pulse conditioning circuits, as well as an analog-to-digital converter (ADC), to convert the analog signals into digital data for processing, as illustrated in Figure 2.

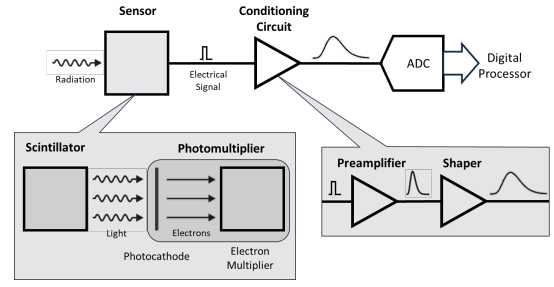The conditioning circuits play a crucial role in shaping the signal to mitigate noise and prepare it for digitization. Finally, the ADC digitizes the signal, making it suitable for storage and detailed analysis using computational tools.

A. Detector

Scintillators and photomultipliers exemplify a type of radiation detection that efficiently converts incoming radiation into detectable light signals and subsequently into electrical pulses. SiPMs are particularly valued photomultipliers for their ability to detect visible light with exceptional precision. They exhibit excellent single photon detection capabilities and superior timing properties, making them ideal for applications requiring single photon counting. These characteristics render SiPMs as promising candidates for specialized uses such as time-correlated single photon counting in physics, among other fields. Although this system is adept at detecting cosmic radiation [10].

When discussing the interaction of scintillators detectors with radiation the temporal behavior of the emitted light is critically important, much like the energy from the interaction itself [11].

The scintillation process is not instantaneous, the light intensity is characterized by a very fast rise time (τ_D) followed by an exponential decay time (τ_R) during the scintillation process. This phenomenon is further combined with the capacitive characteristics of SiPMs, which are also modeled using exponential functions for charge accumulation and discharge decay.

This profile can be effectively modeled by a multi-exponential function, which captures both the rise and decay phases of the light pulse along, with the electrical charging and discharging processes. However, the electrical pulse output from a scintillation detector can be approximated using a bi-exponential function [11], as indicated in the equation:

$$x(t) \propto e^{-t/\tau_D} - e^{-t/\tau_R} \tag{1}$$

B. Conditioning Circuit

Charge Sensitive Amplifier (CSA) acts as a preamplifier to convert the small charge pulses into signals of greater amplitude, corresponding to the electrical charge collected by the detector, making them more easily processable. The shaping circuits extend the duration of the pulses, that $\tau_{R_d C_d}$ is the derivative time constant and $\tau_{R_i C_i}$ is the integral time constant of shaper circuit.. Commonly, they are composed

of a differentiation network followed by one or more signal integration networks, which also characterize other exponential behavior in the signal, exemplified in equation 2. The shapper circuit reduct the necessary sampling rate, as high acquisition rates tend to make the design of the instrument costly and, in more critical cases, render the instrument unfeasible due to the lack of appropriate technology for digitization [4].

$$y(t) \propto (e^{-t/\tau_{R_d} C_d} - e^{-t/\tau_{R_i} C_i}) \, x(t) \qquad (2)$$

Furthermore, it is widely recognized that any measurement system inevitably alters the measured quantity despite efforts to minimize these effects. This phenomenon is particularly relevant in particle detection systems, where both auxiliary components and the sensor introduce modifications to the pulse shape of the measurements. Consequently, understanding and compensating for these changes is essential for improving the performance of pulse detectors [12].

The ADC is considered ideal for modeling the reading system, in which the sampling rate (T_s) is chosen to effortlessly satisfy the Nyquist pulse criterion for digitization. The amplitude resolution is much smaller than the resolution of the set of all components of the reading chain, so it can be neglected. The measurement system's auxiliary components and the detectors themselves are meticulously designed to operate in a linear region. It ensures that the energy deposited by the particle is directly proportional to the number of photons received in the scintillator, which in turn is proportional to the number of electrons generated, and so on in the reading chain.

III. UNFOLDING METHOD FOR MEASUREMENT SYSTEM COMPENSATION

When measuring any quantity, the system changes undesirably despite efforts to ensure that the systems influence the measurements as little as possible. Radiation and particle detection systems fit into this reality. Such realistic measurement conditions encourage using the generalist model of measuring instruments by configuring inputs and outputs [13].

The measurement instrument model considers three types of inputs, which can be scalars or vectors, to represent a set of inputs of the same type [13]:

- $x_d(t)$ is the signal of interest, as it represents the measurement, that is, the true value of the physical quantity being measured;
- $x_m(t)$ is the modifying input, a type of spurious input, which acts on the instrument parameters, changing the measurement system and indirectly changing the measurement indication;
- $x_i(t)$ is the interfering input, another type of spurious input directly affecting the measurement result. The contribution of the interference input is considered to be additive.

Ideally, there is an instrument function ($f\{\cdot\}$) capable of indicating the measurands $y_d(t) = f\{x_d(t)\}$ so that this function is invertible and allows recovery or measuring. However, this function suffers influence by the modifying input and presents another indication:

$$\tilde{f}\{x_d(t)\} = f\{x_d(t), x_m(t)\} \neq y_d(t) \qquad (3)$$

Both the measurement system's auxiliary components and the detectors themselves are designed to operate in a linear region, allowing the model to be approximated by a linear expression. Thus, according to the equation, it is possible to interpret the modifying input as an additive effect and separate it from the measurand.

$$\tilde{f}\{x_d(t)\} = f\{x_d(t)\} + p \cdot f\{x_m(t)\} \qquad (4)$$

where p is a weighting coefficient of the indications provided by each of the inputs.

Similarly to the ideal instrument, but represented in a more "relaxed" way, another instrument ($g\{\cdot\}$) indicates the tampering due to the stimulus of the interfering input. It is also changed by the modifying input ($\tilde{g}\{x_i(t)\}$) .

The output $y(t)$ is the indication of the real instrument, after all input effects are combined, which is mathematically represented by:

$$y(t) = f\{x_d(t)\} + p f\{x_m(t)\} + \tilde{g}\{x_i(t)\} \qquad (5)$$

Given the simplifying assumptions of the measurement system, it is possible to mitigate the effects of modifying inputs and interfering inputs using the unfolding compensation method.

A. Wiener Filter

Linear filtering algorithms estimate a response $\hat{x}[k]$ from N consecutive samples $\mathbf{y}[k] = [y[k], y[k-1], \ldots, y[k-N]]$ using filter weights $\mathbf{w} = [w[0], w[1], \ldots, w[N-1]]^T$ through convolution, where k is the discrete time index, obtained by the continuous time t, by the sample period T_s ($k = t/T_s$). N is the order of the filter. For peak amplitude recovery, an inverse filter, which uses a known pulse shape, optimizes the weights via a Wiener method that follows the principle of data orthogonality [14], minimizing the squared errors as per the cost function in equation:

$$J(\mathbf{w}) = \sum_{k=0}^{K-1} (x[k] - \mathbf{y}[k]\mathbf{w})^2 = (\mathbf{x} - \mathbf{Y}\mathbf{w})(\mathbf{x} - \mathbf{Y}\mathbf{w}) \quad (6)$$

where the observation matrix $\mathbf{Y}$ is formed by the shifted observed signal $\mathbf{y}[k]$ with zero padding and K is the length of signal observation.

The optimal weights are obtained by setting the derivative of the cost function with respect to the weights to zero, as shown in equation:

$$\frac{\partial J}{\partial \mathbf{w}} = -2\mathbf{Y}\mathbf{x} + 2\mathbf{Y}\mathbf{Y}^T\mathbf{w} = 0$$

$$\mathbf{w} = (\mathbf{Y}\mathbf{Y}^T)^{-1}\mathbf{Y}\mathbf{x} \qquad (7)$$

The computation of the weights describes the stage of filter parameterization, and these determined weights are applied to estimate signal samples $\hat{x}_0[k]$, by the equation:

$$\hat{x}_0[k] = \mathbf{y}[k]\mathbf{w} \qquad (8)$$

B. Sparsity Theory

However, addressing noise solely with the Wiener filter requires a filter order that does not necessarily resolve the noise issue. The unfolding problem in noisy environments can be represented using a sparse representation. This involves minimizing the ℓ_1-norm ($||\mathbf{x}||_1$), which promotes sparsity by summing the absolute values of the estimated data samples. Concurrently, fidelity to the original data is maintained by minimizing the squared ℓ_2-norm of the deviation between the estimated and actual data ($||\mathbf{x} - \mathbf{W}\mathbf{y}^{\mathbf{T}}||_2^2$). This optimization problem is simplified into an unconstrained one by choosing an appropriate multiplier λ_0, balancing the sparsity and model fidelity, as the cost function in equation [15]:

$$J(\mathbf{x}) = \lambda_0||\mathbf{x}||_1 + ||\mathbf{x} - \mathbf{W}\mathbf{y}^{\mathbf{T}}||_2^2 \qquad (9)$$

where the deconvolution matrix $\mathbf{W}$ is formed by the weight vector $\mathbf{W}$ shifted line by line with zero padding.

$$\mathbf{W} = \begin{bmatrix} \mathbf{w}^T & 0 & \cdots & 0 \\ 0 & \mathbf{w}^T & \cdots & 0 \\ \vdots & \vdots & \ddots & \vdots \\ 0 & 0 & \cdots & \mathbf{w}^T \end{bmatrix}_{K \times K}$$

.

Only non-negative values of the target vector are allowed in this application, as like photon interactions in scintillating detectors. Therefore, the modulus operation can be neglected. In order to minimize the cost function, ensuring sparsity of estimated samples, the cost function is derived in terms of $\mathbf{x}$ and set equal to zero.

$$\frac{\partial J}{\partial \mathbf{x}} = \lambda_0\mathbf{1} + 2\mathbf{x} - 2\mathbf{W}\mathbf{y}^{\mathbf{T}} = 0$$

$$\mathbf{x} = \mathbf{W}\mathbf{y}^{\mathbf{T}} - \lambda\mathbf{1}, \ \mathbf{x} > 0 \qquad (10)$$

where $\mathbf{1}$ is a column vector of ones.

By decoupling the individual components of the expressions contained in the equation (10), a simplified equation is obtained, that includes the use of a linear filter for unfolding to produce an estimated signal $\hat{x}_0[k] = \mathbf{y}[k]\mathbf{w}$, which is then processed through the application of a conditional threshold to enhance sparsity, accommodating only non-negative values ($x[k] > 0$).

$$\hat{x}_\lambda[k] = \mathbf{y}[k]\mathbf{w} - \lambda, \ \hat{x}_\lambda[k] > 0 \qquad (11)$$

where $\hat{x}_\lambda$ is the sparse estimated signal.

From equation 11, the shrinkage or threshold technique is characterized, that is interpreted as a nonlinear function (S_λ) that is presented in equation (12), and demonstrated in Figure 3 [16]. This function maps values smaller in modulus

than a constant to zero and mantains values outside this range by subtracting them by the constant λ [17].

$$\hat{x}_\lambda[k] = S_\lambda(\hat{x}_0[k]) = \begin{cases} \hat{x}_0[k] - \lambda, & if \ \hat{x}[k] > \lambda, \\ 0, & if \ \hat{x}[k] \leq \lambda \end{cases} \qquad (12)$$
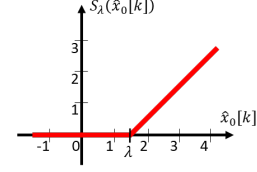

Fig. 3. Example of shrinkage function.

The operation in equation (11) can be understood as a linear filter that performs unfolding and provides an estimated signal $\hat{x}_0[k] = \mathbf{w}_k^T \mathbf{y}_N[k]$, followed by conditional thresholding. It is possible to use the same linear filter computed by the Wiener method. Then, the proposed shrinkage algorithm is applied to the signal estimated by the filter.

The use of the Wiener filter combined to shrinkage technique is particularly interesting in the context of unfolding, where two components of the measurement system must be compensated: both the noise as interfering input, and the modifying inputs of the instrumentation system. This allows for the generation of the inverse system to recover the measurand, which is the input of interest.

IV. RESULTS

This section will present the results obtained through the experimental data, taken from a workbench, applied to the proposed algorithms. First, the system's characteristic pulse will be analyzed, followed by the results of the proposed signal processing techniques applied to the data from our detection system. Two metrics are proposed for analyzing the results: the Standard Deviation (STD) applied to the set of waveform measurements and the Root Mean Square Error (RMSE).

The STD allows us to assess the variability of the waveforms, focusing primarily on the variability of the waveform peak.

Similarly, the RMSE quantifies how close the recovered signals are to the ideal values, providing a straightforward measure of the improvement brought by the implemented techniques. It offers a robust means of comparing the integrity of the signals after processing, ensuring that the modifications introduced by our processing system contribute to the recovery of the maximum waveform peak.

A. Data Acquisition

An experimental setup was developed for the acquisition of cosmic rays, as shown in Figure 4. The setup utilizes two DC voltage sources, one to power the SiPM with a voltage of $55 \ V$ and a symmetric source of $\pm 5 \ V$ to power the amplifiers in the conditioning circuit. The conditioning circuit consists of a charge-sensitive preamplifier and an integrating shaper circuit.
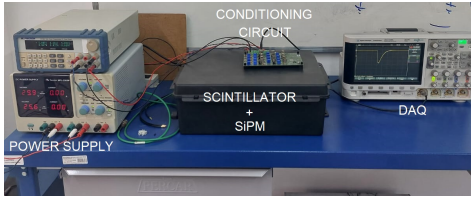
Fig. 4. Workbench.

Fig. 6. Filter order error curve.

The data acquisition system consists of a $200\ MHz$ oscilloscope with a sampling rate of $4\ GSa/s$, that was configured to $T_s = 1\ ns$. The oscilloscope is connected to a computer via USB with a baud rate of $9600\ bits/s$. A LabView program was developed for storing data provided by the experimental setup.

More than 500 pulses from cosmic ray events interacting with the scintillator were collected, but a data cleaning process was necessary that removed entries without pulses, which provided a set of 502 valid pulses. Preliminarily, preprocessing was performed by normalizing all pulses to a range from 0 to 1, which are shown in Figure 5. The normalization is usefull for comparison criterion, as it sets the expected pulse amplitude to 1, providing a reference for calculating the RMSE in parametrization stage.
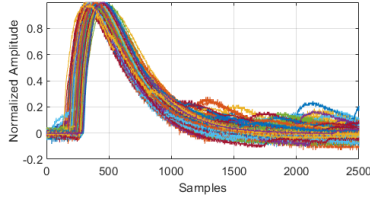

Fig. 5. Acquired Pulses for Analysis.

The mean and standard deviation among the pulses were calculated,that only the STD near the region where the waveform peaks occur is considered. The value in this region is $2.52 \cdot 10^{-2}$.

A set of 300 pulses, constituting 60% of the database, was randomly selected for algorithm parameterization. The remaining 40% of the database, comprising 200 pulses, was selected for testing.

B. Parameters Selection

In this study, the methods were parameterized solely with 60% of the dataset samples organized into 5 separate folds, with the intent of eliminating bias during the selection of parameters and enhancing the reliability of subsequent efficiency comparisons.

The Wiener filter algorithm's design involves selecting just one parameter, the filter order (N). The tuning of the weights is contingent upon the sample pairs. Each time the filter order is changed, the weights are reparameterized, and the resulting RMSE is displayed in Figure 6.

With increasing the filter order beyond 600, there is a degradation of the result, hence $N = 609$ was selected. This
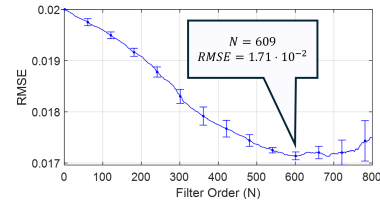
high filter order is primarily due to the noise embedded in the signal, necessitating a high order to adequately address the noise.

After selecting and parameterizing the filter order, determining the sparsity parameter involves setting the threshold value (λ) for the shrinkage algorithm. Figure 7 displays the error curve relative to the threshold value. The figure illustrates that reducing this parameter aligns the results more closely with the Wiener filter, whereas increasing it results in sparser representations, however in a upper limit all samples are zeroed.
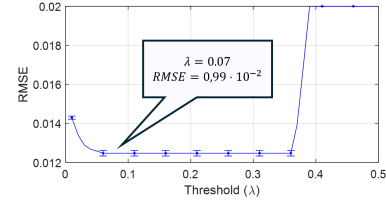

Fig. 7. Threshold error curve.

It is noteworthy that there is a range of threshold values between 0.06 and 0.36 that can be selected, as there is no change in either the mean or the standard deviation of the results. A more conservative choice is a lower threshold value; therefore, $\lambda = 0.07$ was selected.

C. Unfolding Technique Application

With the parameters derived from the dataset, we begin analyzing the algorithm using previously unused data. The evaluation of the algorithm involves applying the proposed unfolding algorithm to each pulse, without normalizing the pulses. The Figure 9 displays the average and standard deviation of the pulses both before and after processing.
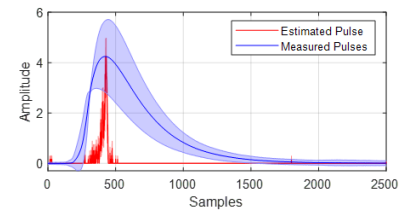

Fig. 8. Comparison of the average pulses without compensation and compensated by the unfolding algorithm.

The peak of the pulses typically occurs around sample 415. By fixing this point, we assess the standard deviation of the

pulse amplitudes without compensation that is 1.44, which is reduced after applying the unfolding algorithm to 0.69. The Figure presents the histogram of the peak sample with and without compensation.
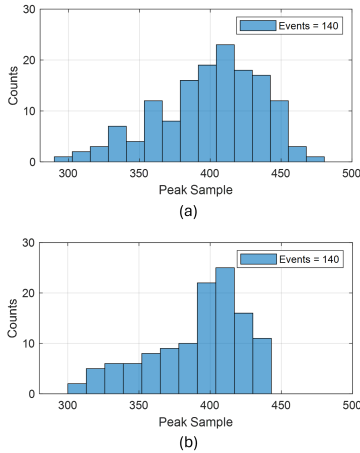

Fig. 9. Histograms comparison of sample peak amplitude: (a) Non compensated and (b) Compensated.

This reduction highlights that the unfolding algorithm provides less variability in the peak heights relative to the pulse position, effectively compensating for the delay until the signal reaches its maximum.

V. Conclusion and Future Works

This study demonstrated the application of the unfolding algorithm, which combines the Wiener Filter and Sparsity theory, to narrow the pulse in time. This approach is aimed at preventing the pile-up effect, even when the pulse is immersed in electronic noise, as the workbench to cosmic rays measurement.

The application of the unfolding algorithm significantly improved the consistency of peak positioning, as evidenced by the reduced variability and standard deviation in the compensated pulses compared to those without compensation.

These improvements are crucial for applications requiring precise radiation detection and measurement. Future work could explore further refinements to the algorithm to optimize its performance across different types of radiation and more complex detection scenarios.

Future studies will aim to incorporate specific denoising techniques in the preprocessing of the signal, using an extended time window to determine if a baseline shift occurs. Additionally, the use of artificial neural networks will be explored for the regression of pulse time and amplitude, potentially enhancing the accuracy and efficiency of the signal analysis process.

Acknowledgment

References

[1] H. Park, M. Yi, and J. S. Lee, "Silicon photomultiplier signal readout and multiplexing techniques for positron emission tomography: a review," *Biomedical engineering letters*, vol. 12, no. 3, pp. 263–283, 2022.

[2] M. Conti and B. Bendriem, "The new opportunities for high time resolution clinical tof pet," *Clinical and Translational Imaging*, vol. 7, no. 2, pp. 139–147, 2019.

[3] H. Spieler, *Semiconductor detector systems*, vol. 12. Oxford university press, 2005.

[4] H. Spieler, "Pulse processing and analysis," in *IEEE Nuclear Science Symposium Short Course*, (San Francisco), pp. 52–90, IEEE, 2002.

[5] V. T. Jordanov, "Deconvolution of pulses from a detector-amplifier configuration," *Nuc. Instrum. Methods in Phys. Res. A*, vol. 351, no. 2-3, pp. 592–594, 1994.

[6] V. T. Jordanov, "Unfolding-synthesis technique for digital pulse processing. part 1: Unfolding," *Nuclear Instruments and Methods in Physics Research Section A: Accelerators, Spectrometers, Detectors and Associated Equipment*, vol. 805, pp. 63–71, 2016.

[7] A. Di Fulvio, T. Shin, M. Hamel, and S. Pozzi, "Digital pulse processing for nai (tl) detectors," *Nuc. Instrum. Methods in Phys. Res. A*, vol. 806, pp. 169–174, 2016.

[8] G.-Q. Zeng, J. Yang, M.-F. Yu, K.-Q. Zhang, Q. Ge, and L.-Q. Ge, "Digital pulse deconvolution method for current tails of nai (tl) detectors," *Chin. Phys. C*, vol. 41, no. 1, p. 016102, 2017.

[9] T. M. Quirino and L. M. de Andrade Filho, "Non-negative sparse deconvolution method for PMT signals in radiation detectors," *Nucl. Instrum. Meth. A*, vol. 1061, p. 169142, 2024.

[10] J. G. Webster and H. Eren, *Measurement, instrumentation, and sensors handbook: spatial, mechanical, thermal, and radiation measurement*. CRC press, 2017.

[11] S. Gundacker and A. Heering, "The silicon photomultiplier: fundamentals and applications of a modern solid-state photon detector," *Physics in Medicine & Biology*, vol. 65, no. 17, p. 17TR01, 2020.

[12] G. F. Knoll, *Radiation detection and measurement*. New Jersey: John Wiley & Sons, 2010.

[13] E. Doebelin, *Instrumentation design studies*. Crc Press, 2010.

[14] S. S. Haykin, *Adaptive Filter Theory*. New Jersey: Prentice Hall, 3 ed., 1996.

[15] M. Elad, *Sparse and redundant representations: from theory to applications in signal and image processing*. Berlin: Springer Science & Business Media, 2010.

[16] T. Boas, A. Dutta, X. Li, K. P. Mercier, and E. Niderman, "Shrinkage function and its applications in matrix approximation," *arXiv preprint arXiv:1601.07600*, 2016.

[17] D. L. Donoho, "De-noising by soft-thresholding," *IEEE Trans. Inf. Theory*, vol. 41, no. 3, pp. 613–627, 1995.